Results Math (2023) 78:53
Online First

https://doi.org/10.1007/s00025-022-01831-0
Results in Mathematics

Generalized Henneberg Stable Minimal Surfaces

David Moya and Joaquín Pérez

Abstract. We generalize the classical Henneberg minimal surface by giving an infinite family of complete, finitely branched, non-orientable, stable minimal surfaces in $\mathbb{R}^3$. These surfaces can be grouped into subfamilies depending on a positive integer (called the *complexity*), which essentially measures the number of branch points. The classical Henneberg surface H_1 is characterized as the unique example in the subfamily of the simplest complexity $m = 1$, while for $m \geq 2$ multiparameter families are given. The isometry group of the most symmetric example H_m with a given complexity $m \in \mathbb{N}$ is either isomorphic to the dihedral isometry group D_{2m+2} (if m is odd) or to $D_{m+1} \times \mathbb{Z}_2$ (if m is even). Furthermore, for m even H_m is the unique solution to the Björling problem for a hypocycloid of $m + 1$ cusps (if m is even), while for m odd the conjugate minimal surface H^*_m to H_m is the unique solution to the Björling problem for a hypocycloid of $2m + 2$ cusps.

1. Introduction

A celebrated result obtained independently by do Carmo and Peng [1], Fischer-Colbrie and Schoen [2] and Pogorelov [7] establishes that if M is a complete orientable stable minimal surface in $\mathbb{R}^3$, then M is a plane. Ros [8] proved that the same characterization holds without assuming orientability. Nevertheless, a plethora of complete stable minimal surfaces in $\mathbb{R}^3$ appear if we allow these stable minimal surfaces to have branch points, with the simplest example being the classical Henneberg minimal surface [3].

The class of complete, finitely connected and finitely branched minimal surfaces with finite total curvature (among which stable ones are a particular case) appears naturally in the following situation: Given $\varepsilon_0 > 0$, $I \in \mathbb{N} \cup \{0\}$

Published online: 09 January 2023

and $H_0, K_0 \geq 0$, let $\Lambda = \Lambda(I, H_0, \varepsilon_0, K_0)$ be the set of immersions $F: M \looparrowright X$ where X is a complete Riemannian 3-manifold with injectivity radius $\text{Inj}(X) \geq \varepsilon_0$ and absolute sectional curvature bounded from above by K_0, M is a complete surface, F has constant mean curvature $H \in [0, H_0]$ and Morse index at most I. The second fundamental form $|A_{F_n}|$ of a sequence $\{F_n\}_n \subset \Lambda$ may fail to be uniformly bounded, which leads to lack of compactness of Λ. Nevertheless, the interesting ambient geometry of the immersions F_n can be proven to be well organized locally around at most I points $p_{1,n}, \ldots, p_{k,n} \in M_n$ $(k \leq I)$ where $|A_{F_n}|$ takes on arbitrarily large local maximum values. Around any of these points $p_{i,n}$, one can perform a blow-up analysis and find a limit of (a subsequence of) expansions $\lambda_n F_n$ of the F_n (that is, we view F_n as an immersion with constant mean curvature H_n/λ_n in the scaled ambient manifold $\lambda_n X_n$ for a sequence $\{\lambda_n\}_n \subset \mathbb{R}^+$ tending to ∞). This limit is a complete immersed minimal surface $f: \Sigma \looparrowright \mathbb{R}^3$ with finite total curvature, passing through the origin $\vec{0} \in \mathbb{R}^3$. Recall that such an f has finitely many ends, each of which is a multi-valued graph of finite multiplicity (spinning) $s \in \mathbb{N}$, over the exterior of a disk in the tangent plane at infinite for f at that end. Thus, arbitrarily small almost perfectly formed copies of large compact portions of $f(\Sigma)$ can be reproduced in $F_n(M_n)$ around $F_n(p_{i,n})$ for n sufficiently large. Complete, finitely-connected and finitely-branched minimal surfaces with finite total curvature in $\mathbb{R}^3$ appear naturally when considering clustering phenomena in this framework: It may occur that different blow-up limits of the F_n around $p_{i,n}$ at different scales $\lambda_{1,n} > \lambda_{2,n}$ with $\lambda_{1,n}/\lambda_{2,n} \to \infty$ as $n \to \infty$, produce different limits $f_j: \Sigma_j \looparrowright \mathbb{R}^3$, $j = 1, 2$, with $\text{Index}(f_1) + \text{Index}(f_2) \leq I$; in this case, all the geometry of $f_1(\Sigma_1)$ collapses around $\vec{0} \in f_2(\Sigma_2)$, and every end of $f_1(\Sigma_1)$ with multiplicity $m \geq 3$ produces a branch point at the origin for $f_2(\Sigma_2)$ of branching order $s - 1$. For details about this clustering phenomenon and how to organize these blow-up limits in hierarchies appearing around $\{p_{i,n}\}_n$, see the paper [4] by Meeks and the second author.

The main goal of this paper is to generalize the classical Henneberg minimal surface H_1 to an infinite family of connected, 1-sided, complete, finitely branched, stable minimal surfaces in $\mathbb{R}^3$. Branch points are unavoidable if we seek for complete, non-flat stable minimal surfaces by the aforementioned results [1,2,7,8]; 1-sidedness is also necessary condition for stability (see Proposition 3 below). Our examples can be grouped into subfamilies depending on the number of branch points (this will be encoded by an integer $m \in \mathbb{N}$ called the *complexity*). The most symmetric examples H_m in each subfamily of complexity m will be studied in depth (Sect. 5.3). Depending on the parity of m, either H_m or its conjugate minimal surface H_m^* (which does not gives rise to a 1-sided surface, see Sect. 5.4) can be viewed as the unique solution of a Björling problem for a planar hypocycloid (Sect. 5.7). The isometry group of H_m is isomorphic to the dihedral group D_{2m+2} if m is odd and to the group $D_{m+1} \times \mathbb{Z}_2$ if m is even (Sect. 5.8). We will also prove that H_1 is the only element in the subfamily with complexity $m = 1$ (Theorem 11), while for $m \geq 2$, H_m can be deformed in multiparameter families: Proposition 14 gives an explicit 1-parameter family of examples with complexity $m = 2$, interpolating between H_2 and a limit which turns out to be H_1 (Sect. 6.2.1), and the subfamily of examples with complexity $m = 2$ is a two-dimensional real analytic manifold around H_2 (Sect. 6.2.2).

2. 1-Sided Branched Stable Minimal Surfaces

We start with the Weierstrass data (g, ω) on a Riemann surface Σ, so that (g, ω) solves the period problem and produces a conformal harmonic map $X : \Sigma \looparrowright \mathbb{R}^3$ given by the classical formula

$$X = \mathrm{Re} \int (\phi_1, \phi_2, \phi_3) = \mathrm{Re} \int \left(\frac{1}{2}(1 - g^2)\omega, \frac{i}{2}(1 + g^2)\omega, g\omega \right). \tag{1}$$

We will assume that X is an immersion outside of a locally finite set of points $\mathcal{B} \subset \Sigma$, where X fails to be an immersion (points of $\mathcal{B}$ are called *branch points* of X). Such an X will be called a *branched minimal immersion*. The induced (possible branched) metric is given by

$$ds^2 = \frac{1}{4}(1 + |g|^2)^2 |\omega|^2. \tag{2}$$

The local structure of X around a branch point in $\mathcal{B}$ is well-known, see e.g. Micallef and White [5, Theorem 1.4] for details. Given $p \in \mathcal{B}$, there exists a conformal coordinate (D, z) for Σ centered at p (here D is the closed unit disk in the plane), a diffeomorphism u of D and a rotation ϕ of $\mathbb{R}^3$ such that $\phi \circ X \circ u$ has the form

$$z \mapsto (z^q, x(z)) \in \mathbb{C} \times \mathbb{R} \sim \mathbb{R}^3$$

for z near 0, where $q \in \mathbb{N}$, $q \geq 2$, x is of class C^2, and $x(z) = o(|z|^q)$. In this setting, the *branching order of* p is defined to be $q - 1 \in \mathbb{N}$.

Let us assume that X produces a 1-sided branched minimal surface; this means that there exists an anti-holomorphic involution without fixed points $I : \Sigma \to \Sigma$ such that $I \circ \phi_j = \overline{\phi_j}$ for $j = 1, 2, 3$. This is equivalent to

$$-1/\overline{g} = g \circ I, \qquad I^* \omega = -\overline{g^2 \omega}. \tag{3}$$

In particular, I must preserve the set $\mathcal{B}$. $\Sigma/\langle I \rangle$ is a non-orientable differentiable surface endowed with a conformal class of metrics, and the harmonic map X induces another harmonic map $\widehat{X} : \Sigma/\langle I \rangle \looparrowright \mathbb{R}^3$ such that $\widehat{X} \circ \pi = X$, where $\pi : \Sigma \to \Sigma/\langle I \rangle$ is the natural projection ($\widehat{X}$ is a branched minimal immersion). Reciprocally, every 1-sided conformal harmonic map can be constructed in this way.

Remark 1. In the particular case that the compactification of Σ is $\overline{\mathbb{C}}$, we can assume that $I(z) = -1/\overline{z}$ and write $\omega = f\,dz$ globally. In this setting, the above equations give

$$-1/\overline{g(z)} = g(-1/\overline{z}), \quad f \circ I = -\overline{z^2 g^2 f}. \tag{4}$$

Definition 2. Given a 1-sided conformal harmonic map $\widehat{X}\colon \Sigma/\langle I\rangle \looparrowright \mathbb{R}^3$, we denote by Δ, $|A|^2$ the Laplacian and squared norm of the second fundamental form of $\widehat{X}$. The *index* of $\widehat{X}$ is defined as the number of negative eigenvalues of the elliptic, self-adjoint operator $L = \Delta + |A|^2$ (Jacobi operator of X) defined over the space of compactly supported smooth functions $\phi\colon \Sigma \to \mathbb{R}$ such that $\phi \circ I = -\phi$. $\widehat{X}$ is said to be *stable* if its index is zero.

In the case $\widehat{X}$ is finitely branched, the eigenvalues and eigenfunctions of the Jacobi operator of X are well defined via a variational approach, since the codimension of the singularity set $\mathcal{B}$ is two (see [9]), and stability also makes sense.

The next result is proven by Meeks and the second author in [4].

Proposition 3. *Let $X\colon \Sigma \looparrowright \mathbb{R}^3$ be complete, non-flat, finitely branched minimal immersion with branch locus $\mathcal{B} \subset \Sigma$. Then:*

1. *[4, Proposition 3] If X is stable, then Σ is non-orientable and $X(\mathcal{B})$ contains more than 1 point.*
2. *[4, Remark 3.6] Suppose that Σ is non-orientable, X has finite total curvature and its extended unoriented Gauss map $G\colon \mathbb{P}^2 = \mathbb{S}^2/\{\pm 1\} \to \mathbb{P}^2$ is a diffeomorphism. Then, X is stable.*

3. The Björling Problem

We next recall the basics of the classical Björling problem, to be used later. Let $\gamma\colon I \subset \mathbb{R} \to \mathbb{R}^3$ be an analytic regular curve and η an analytic vector field along γ such that $\langle \gamma(t), \eta(t)\rangle = 0$ and $\|\eta(t)\| = 1$ for all $t \in I$. The classical result due to E.G. Björling asserts that the following parametrization generates a minimal surface S which contains γ and has η as unit normal vector along γ:

$$X(u,v) = \operatorname{Re}\left(\widetilde{\gamma}(w) - i\int_{w_0}^{w} \widetilde{\eta}(w) \times \widetilde{\gamma}'(w)\,dw\right),$$

where $\widetilde{\gamma}, \widetilde{\eta}$ are analytic extensions of the corresponding γ, η and $w = u + iv$ is defined in a simply connected domain $\Omega \subset \mathbb{C}$ with $I \subset \Omega$. In particular, the surface S is locally unique around γ with this data (it is called the solution to the Björling problem with data γ, η).

In what follows, we will consider different Björling problems for analytic planar curves $\gamma \subset \{z = 0\}$ that fail to be regular at finitely many points. The above construction can be applied to each of the regular arcs of these curves after removing the zeros of γ'. In all our applications, η will be taken as the (unit) normal vector field to γ as a planar curve.

4. The Classical Henneberg Surface

The classical Henneberg minimal surface H_1 is the 1-sided, complete, stable minimal surface in $\mathbb{R}^3$ given by the Weierstrass data:

$$g(z) = z, \quad \omega = z^{-4}(z \pm i)(z \pm 1)dz = z^{-4}(z^4 - 1)dz, \quad z \in \overline{\mathbb{C}} - \{0, \infty\}. \tag{5}$$

H_1 has two branch points[1] at $[1] = \{1, -1\}, [i] = \{i, -i\} \in \mathbb{P}^2 = \overline{\mathbb{C}}/\langle A \rangle$, where $A(z) = -1/\overline{z}$ is the antipodal map. By Proposition 3, H_1 is stable.

H_1 can be conformally parameterized (up to translations) by eq. (1). After translating X so that $X(e^{i\pi/4}) = \vec{0}$, the branch points of H_1 are mapped by X to $(0, 0, \pm 1)$ and a parametrization of H_1 in polar coordinates $z = re^{i\theta}$ is given by

$$X(re^{i\theta}) = \begin{pmatrix} \frac{\cos\theta}{2}(r - \frac{1}{r}) - \frac{\cos(3\theta)}{6}(r^3 - \frac{1}{r^3}) \\ -\frac{\sin\theta}{2}(r - \frac{1}{r}) - \frac{\sin(3\theta)}{6}(r^3 - \frac{1}{r^3}) \\ \frac{\cos(2\theta)}{2}(r^2 + \frac{1}{r^2}) \end{pmatrix}. \tag{6}$$

Since $X(e^{i\theta}) = (0, 0, \cos(2\theta))$, then X maps the unit circle into the vertical segment $\{(0, 0, t) | \, t \in [-1, 1]\}$. In this way, $\theta \in [0, 2\pi] \mapsto X(e^{i\theta})$ bounces between the two branch points of H_1 (observe that the complement of this closed segment in the x_3-axis is not contained in H_1), see Fig. 1.

4.1. Isometries of H_1

It is straightforward to check that

1. The antipodal map $A\colon \overline{\mathbb{C}} \to \overline{\mathbb{C}}$ (in polar coordinates $(r, \theta) \mapsto (1/r, \pi + \theta)$) leaves the surface invariant. This is the deck transformation, which is orientation reversing.
2. The map $z \mapsto -z$ (in polar coordinates $(r, \theta) \mapsto (r, \pi + \theta)$) induces the rotation by angle π about the axis x_3 on the surface.
3. The inversion of the z-plane with respect to the unit circle, $z \mapsto 1/z$, (in polar coordinates $(r, \theta) \mapsto (1/r, \theta)$) is the composition of A with $z \mapsto -z$, and thus, it also induces a rotation of angle π about the x_3-axis on the surface.
4. The conjugation map $z \mapsto \overline{z}$ (in polar coordinates $(r, \theta) \mapsto (r, -\theta)$) induces the reflection of X about the plane (x_1, x_3).
5. The reflection about the imaginary axis (in polar coordinates $(r, \theta) \mapsto (r, \pi - \theta)$) induces the reflection of X about the plane (x_2, x_3).

[1] Branch points of H_1 all have order 1 (locally the surface winds twice around the branch point); this follows from direct computation, or from Proposition 21 in White' s "Lectures on minimal surfaces theory".

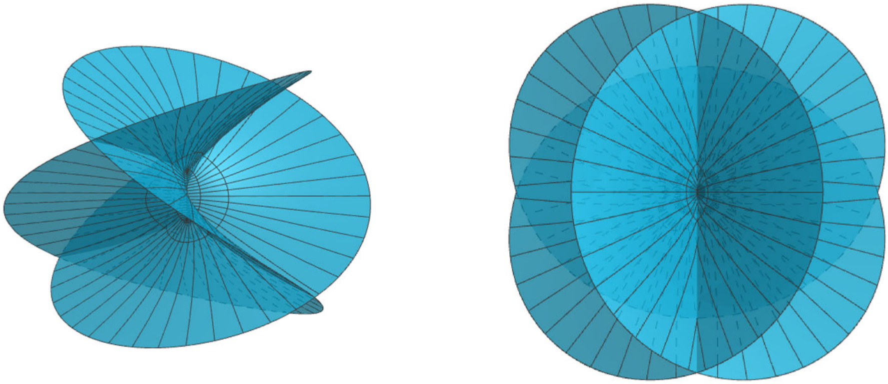

FIGURE 1. The Henneberg surface H_1. After a translation, the branch points of H_1 are contained in the x_3-axis. H_1 contains two horizontal, orthogonal lines that bisect the x_1- and x_2-axis. Left: Intersection of H_1 with a ball of radius 8. Right: top view of H_1

6. X maps the half-line $\{re^{-i\pi/4} \mid r \in (0,\infty)\}$ (respectively $\{re^{i\pi/4} \mid r \in (0,\infty)\}$) injectively into $l_1 = \text{Span}(1,1,0)$ (respectively $l_2 = \text{Span}$ $(1,-1,0)$). Thus, the rotations R_1, R_2 of angle π about l_1, l_2 are isometries of X (R_1 is induced by $z \mapsto -i\overline{z}$ and R_2 by $z \mapsto i\overline{z}$).
7. The map $z \mapsto iz$ (in polar coordinates $(r,\theta) \mapsto (r, \theta + \pi/2)$) induces the rotation of angle $\pi/2$ about the x_3-axis composed by a reflection in the (x_1, x_2)-plane.

Together with the identity map, the above isometries form a subgroup of the isometry group $\text{Iso}(H_1)$ of H_1, isomorphic to the dihedral group D_4.

Lemma 4. *These are all the (intrinsic) isometries of* H_1.

Proof. This is a direct consequence of the fact that every intrinsic isometry ϕ of H_1 produces a conformal diffeomorphism of $\mathbb{C}\setminus\{0\}$ into itself that preserves the set of branch points of H_1. In particular ϕ is of one of the aforementioned eight cases. □

4.2. Associated Family and the Conjugate Surface H_1^*

The flux vector of H_1 around the origin in $\mathbb{C}$ vanishes (in other words, the Weierstrass form $\Phi = (\phi_1, \phi_2, \phi_3)$ associated to H_1 is exact). This implies that all associated surfaces $\{\widetilde{H}_1(\varphi) \mid \varphi \in [0, 2\pi)\}$ to the orientable cover $\widetilde{H}_1 = \widetilde{H}_1(0)$ of H_1 are well-defined as surfaces in $\mathbb{R}^3$ (the branched minimal immersion $\widetilde{H}_1(\varphi)$ has Weierstrass data $g_\varphi = g$, $\omega_\varphi = e^{i\varphi}\omega$ and it is isometric to $\widetilde{H}_1$, in particular it has the same branch locus as $\widetilde{H}_1$).

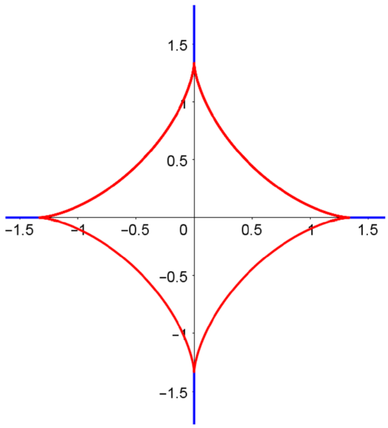

FIGURE 2. The astroid γ_4 (red) and the four rays obtained by intersecting H_1^* with the (x_1, x_2)-plane (blue) (Color figure online)

None of the surfaces $\widetilde{H}_1(\varphi)$ except for $\varphi = 0$ descends to the non-orientable quotient $\mathbb{P}^2\backslash\{[0]\}$, because the second equation in (3) is not preserved if we exchange ω by $e^{i\varphi}\omega$, $\varphi \in (0, 2\pi)$. In particular, none of these associated surfaces are congruent to H_1.

The conjugate surface $H_1^* := \widetilde{H}_1(\pi/2)$ is symmetric by reflection in the (x_1, x_2)-plane. The intersection between H_1^* and $\{z = 0\}$ consists of the *astroid* γ_4 parameterized by

$$t \mapsto \gamma_4(t) = \begin{pmatrix} -\sin(\theta) + \frac{\sin(3\theta)}{3} \\ -\cos(\theta) - \frac{\cos(3\theta)}{3} \\ 0 \end{pmatrix},$$

together with four rays starting at the cusps of the astroid in the direction of their position vectors, see Fig. 2.

In particular, H_1^* is the solution of the Björling problem for the curve γ_4 and the choice of unit normal field the normal vector to γ_4 as a planar curve, see also Remark 8 below.

5. Generalized Henneberg Surfaces

We will next search for a 1-sided, complete, stable minimal surface in $X\colon \Sigma \looparrowright \mathbb{R}^3$ with $\Sigma = \overline{\mathbb{C}}\backslash\mathcal{E}$, $\mathcal{E}$ finite and $g(z) = z$. Hence, $I(z) = -1/\overline{z}$, $\widehat{X} = X/\langle I\rangle\colon \Sigma/\langle I\rangle \looparrowright \mathbb{R}^3$ is stable and (4) writes

$$f(-1/\overline{z}) = -\overline{z^4 f(z)}. \tag{7}$$

5.1. General form for f

We take a general rational function

$$f(z) = \frac{c}{z^{m+3}} \frac{\prod_{j=1}^{M}(z-a_j)}{\prod_{j=1}^{N}(z-b_j)}, \tag{8}$$

where $c, a_j, b_j \in \mathbb{C}^*$, $m \in \mathbb{N}$, $M, N \in \mathbb{N} \cup \{0\}$ are to be determined.

Remark 5. 1. Hennerberg's surface H_1 has $f(z) = z^{-4}(z^4 - 1)$, hence $c = 1$, $m = 1$, $N = 0$, $M = 4$, $\{a_j\} = \{\pm 1, \pm i\}$.
2. The zeros of the induced the metric (2) (branch points of the surface) occur precisely at the points a_j; the ends occur at $0, \infty$ and at the points b_j (in particular, both families $\{a_j\}_j, \{b_j\}_j$ must then come in pairs of antipodal points, see also (12) below).
3. A consequence of the last observation is that when the above rotations in $\mathbb{R}^3$ of our surfaces (provided that the Weierstrass data close periods) are not allowed unless the axis of rotation is vertical.

Imposing (7) to (8) we get

$$c(-1)^{m-1+M-N}\overline{z}^{3+m-M+N} \frac{\prod_{j=1}^{M}(1+a_j\overline{z})}{\prod_{j=1}^{N}(1+b_j\overline{z})} = f(-1/\overline{z}) = -\overline{z^4 f(z)}$$

$$= -\frac{\overline{c}}{\overline{z}^{m-1}} \frac{\prod_{j=1}^{M}(\overline{z}-\overline{a_j})}{\prod_{j=1}^{N}(\overline{z}-\overline{b_j})},$$

thus

$$\overline{c}(-1)^{m+M-N} z^{2+2m-M+N} \prod_{j=1}^{M}(1+\overline{a_j}z) \prod_{j=1}^{N}(z-b_j) = c \prod_{j=1}^{M}(z-a_j) \prod_{j=1}^{N}(1-\overline{b_j}z), \tag{9}$$

from where we deduce that

$$2 + 2m - M + N = 0, \tag{10}$$

in particular $M - N$ is even. Substituting $z = 0$ in (9) we get

$$\overline{c}(-1)^m \prod_{j=1}^{N} b_j = c \prod_{j=1}^{M} a_j. \tag{11}$$

Using (11), we can rewrite (9) as an equality between monic polynomials in z:

$$\prod_{j=1}^{M}\left(\frac{1}{\overline{a_j}} + z\right) \prod_{j=1}^{N}(z-b_j) = \prod_{j=1}^{M}(z-a_j) \prod_{j=1}^{N}\left(\frac{1}{\overline{b_j}} + z\right),$$

from where we deduce that

$$\{a_1,\ldots,a_M\}=\{-1/\overline{a_1},\ldots,-1/\overline{a_M}\},\quad \{b_1,\ldots,b_N\}=\{-1/\overline{b_1},\ldots,-1/\overline{b_N}\}. \tag{12}$$

that is, M,N are even, the a_j (resp. b_j) are given by $M/2$ (resp. $N/2$) pairs of antipodal points in $\mathbb{C}^*$. Now (10) and (11) give respectively:

$$1+m-\widetilde{M}+\widetilde{N}=0, \tag{13}$$

$$-\overline{c}\prod_{j=1}^{N/2}\frac{b_j}{\overline{b_j}}=c\prod_{j=1}^{M/2}\frac{a_j}{\overline{a_j}}. \tag{14}$$

5.2. Solving the Period Problem in the One-Ended Case: Complexity

From (3) and (8) we see that the points where ds^2 can blow up are $z=0,b_1,\ldots,b_N$ and its antipodal points. In order to keep the computations simple, we will assume there are no b_j's, i.e. $N=0$ (or equivalently $M/2=m+1$), which reduces the period problem to imposing

$$\overline{\int_\gamma g^2\omega}=\int_\gamma \omega,\qquad \mathrm{Re}\int_\gamma g\omega=0,$$

where $\gamma=\{|z|=1\}$, or equivalently,

$$\overline{\mathrm{Res}_0(g^2f)}=-\mathrm{Res}_0(f),\quad \mathrm{Im}\,\mathrm{Res}_0(gf)=0. \tag{15}$$

We can simplify (8) to

$$f(z)=\frac{c}{z^{m+3}}\prod_{j=1}^{m+1}(z-a_j)\left(z+\frac{1}{\overline{a_j}}\right), \tag{16}$$

which satisfies (7) (this is the condition to descend to the quotient as a 1-sided surface, provided that the period problem (15) is solved) if and only if (14) holds, which in this case reduces to

$$-\frac{\overline{c}}{c}=\prod_{j=1}^{m+1}\frac{a_j}{\overline{a_j}}. \tag{17}$$

We call

$$P(z):=\prod_{j=1}^{m+1}(z-a_j)\left(z+\frac{1}{\overline{a_j}}\right)=\sum_{h=0}^{2m+2}A_h z^h. \tag{18}$$

Thus,

$$\begin{aligned}\mathrm{Res}_0(f) = c\,\mathrm{Res}_0\left(\sum_{h=0}^{2m+2} A_h z^{h-m-3}\right) = cA_{m+2},\\ \mathrm{Res}_0(g^2 f) = c\,\mathrm{Res}_0\left(\sum_{h=0}^{2m+2} A_h z^{h-m-1}\right) = cA_m,\\ \mathrm{Res}_0(gf) = c\,\mathrm{Res}_0\left(\sum_{h=0}^{2m+2} A_h z^{h-m-2}\right) = cA_{m+1}.\end{aligned}$$

Thus, (15) reduces to

$$\overline{cA_m} = -cA_{m+2}, \quad \mathrm{Im}(cA_{m+1}) = 0. \tag{19}$$

Remark 6. We can assume $|c| = 1$ due to the fact that multiplying the Weierstrass form by a positive number just multiplies the resulting surface by a homothety. Similarly, exchanging c by $-c$ doesn't change the period problem.

We also write $a_j = |a_j|e^{i\theta_j}$, $\theta_j \in \mathbb{R}$. Thus,

$$-a_j + \frac{1}{\overline{a_j}} = \left(-|a_j| + \frac{1}{|a_j|}\right)e^{i\theta_j}, \quad \frac{a_j}{\overline{a_j}} = e^{2i\theta_j},$$

and so,

$$P(z) = \prod_{j=1}^{m+1}\left(z^2 + \left(-|a_j| + \frac{1}{|a_j|}\right)e^{i\theta_j} z - e^{2i\theta_j}\right) \tag{20}$$

Definition 7. Given $m \in \mathbb{N}$, a list $(c, a_1, \ldots, a_{m+1}) \in \mathbb{S}^1 \times (\mathbb{C}^*)^{m+1}$ solving the equations (17),(19) will be called a *solution of the period problem with complexity* m. Note that geometrically, $a_1, \ldots, a_{m+1}$ are the Gaussian images of the branch points of the resulting surface.

5.3. The Case When the a_j are the $(2m+2)$-Roots of Unity

For each complexity m, there is a most symmetric configuration that gives rise to a solution of the period problem for that complexity, which we describe next.

Take the a_j as the solutions of the equation $a^{2m+2} = 1$ (i.e. $|a_j| = 1$ and $\theta_j = \frac{\pi}{m+1}(j-1)$, $j = 1, \ldots, m+1$). Observe that

$$\prod_{j=1}^{m+1}\frac{a_j}{\overline{a_j}} = \prod_{j=1}^{m+1} e^{2i\theta_j} = e^{2i\sum_{j=1}^{m+1}\theta_j} = e^{\frac{2\pi i}{m+1}\sum_{j=1}^{m+1}(j-1)} = e^{\frac{2\pi i}{m+1}\frac{m(m+1)}{2}} = e^{i\pi m},$$

hence the validity of (17) is equivalent in this case to

$$c = \pm i^{m-1}. \tag{21}$$

As for equation (19), note that (20) can be written as

$$P(z) = \prod_{j=1}^{m+1} \left(z^2 - e^{2i\theta_j}\right) = z^{2m+2} - 1,$$

and thus $A_m = 0$ (because $m > 0$), $A_{m+2} = 0$ (because $m + 2 < 2m + 2$) and $A_{m+1} = 0$. In particular, (19) is trivially satisfied for each value of $c \in \mathbb{C}^*$. Therefore, the Weierstrass data

$$g(z) = z, \quad \omega = i^{m-1} z^{-m-3}(z^{2m+2} - 1)dz, \qquad z \in \mathbb{C}^*, \tag{22}$$

give rise to a 1-sided, complete, stable minimal surface H_m. For $m = 1$ we recover the classical Henneberg's surface. Therefore we can view H_m as a natural generalization of the Henneberg surface, from which the title of the paper is derived.

5.4. Associated Family and the Conjugate Surface H_m^*

Since $A_m = A_{m+1} = A_{m+2} = 0$, the flux vector of H_m around the origin in $\mathbb{C}$ vanishes and the Weierstrass form $\Phi = (\phi_1, \phi_2, \phi_3)$ associated to H_m is exact. Thus all associated surfaces $\{\widetilde{H}_m(\varphi) \mid \varphi \in [0, 2\pi)\}$ to the orientable cover $\widetilde{H}_m = \widetilde{H}_m(0)$ of H_m are well-defined. As in the case $m = 1$ (see Sect. 4.2), none of these associated surfaces descends to the 1-sided quotient, except for $\pm H_m$. Let $H_m^* := \widetilde{H}_m(\pi/2)$ be the conjugate surface to H_m.

The behavior of H_m is very different depending on the parity of m. A naive justification of this dependence on the parity of m comes from the fact that the coefficient for ω changes from ± 1 for m odd to $\pm i$ for m even. A more geometric interpretation of this dependence will be given next.

5.5. The Case m Odd

If $m \in \mathbb{N}$ is odd, (22) gives $\omega = z^{-m-3}(z^{2m+2} - 1)dz$. Although H_m has $m+1$ branch points in $\Sigma = \mathbb{P}^2 \setminus \{[0]\}$ (the classes of the $(2m+2)$-roots of unity under the antipodal map), they are mapped into just two different points in $\mathbb{R}^3$: after translating the surface in $\mathbb{R}^3$ so that $X(e^{i\frac{\pi}{2(m+1)}}) = \vec{0}$ (we are using the notation in (1)), the branch points of H_m are mapped to $(0, 0, \pm 1)$ and a parameterization of H_m in polar coordinates is (compare with (6))

$$X(re^{i\theta}) = \begin{pmatrix} x_1 \\ x_2 \\ x_3 \end{pmatrix} = \begin{pmatrix} \frac{\cos(m\theta)}{2m}\left(r^m - \frac{1}{r^m}\right) - \frac{\cos((m+2)\theta)}{2(m+2)}\left(r^{m+2} - \frac{1}{r^{m+2}}\right) \\ -\frac{\sin(m\theta)}{2m}\left(r^m - \frac{1}{r^m}\right) - \frac{\sin((m+2)\theta)}{2(m+2)}\left(r^{m+2} - \frac{1}{r^{m+2}}\right) \\ \frac{\cos((m+1)\theta)}{m+1}\left(r^{m+1} + \frac{1}{r^{m+1}}\right) \end{pmatrix}. \tag{23}$$

X maps the unit circle into the vertical segment $\{(0, 0, t) | t \in [-1, 1]\}$. $\theta \in [0, 2\pi] \mapsto X(e^{i\theta})$ bounces between the two branch points of H_m, and the complement of this closed segment in the x_3-axis is not contained in H_m. $H_m \cap \{x_3 = 0\}$ consists of an equiangular system of $m + 1$ straight lines

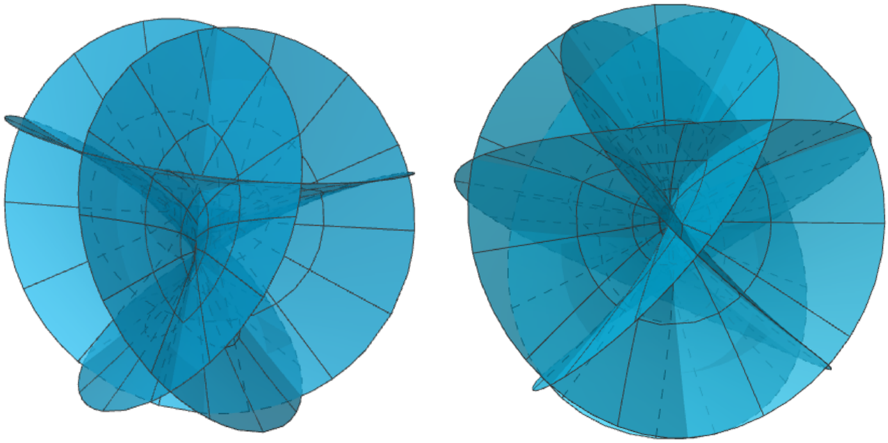

FIGURE 3. Left: H_2. Right: H_3

passing through the origin (the images by X of the straight lines of arguments $\theta = \frac{\pi/2+k\pi}{m+1}$, $k = 0, \dots, m$ in polar coordinates), see Fig. 3 right for H_3.

5.6. The Case m Even

If m is even (and non-zero), (22) produces $\omega = i\, z^{-m-3}(z^{2\,m+2} - 1)dz$. In this case, a parametrization of H_m in polar coordinates is

$$X(re^{i\theta}) = \begin{pmatrix} x_1 \\ x_2 \\ x_3 \end{pmatrix} = \begin{pmatrix} -\frac{\sin(m\theta)}{2m}\left(r^m + \frac{1}{r^m}\right) + \frac{\sin((m+2)\theta)}{2(m+2)}\left(r^{m+2} + \frac{1}{r^{m+2}}\right) \\ -\frac{\cos(m\theta)}{2m}\left(r^m + \frac{1}{r^m}\right) - \frac{\cos((m+2)\theta)}{2(m+2)}\left(r^{m+2} + \frac{1}{r^{m+2}}\right) \\ \frac{\sin((m+1)\theta)}{m+1}\left(\frac{1}{r^{m+1}} - r^{m+1}\right) \end{pmatrix}. \tag{24}$$

X maps the unit circle $\{r = 1\}$ into a certain hypocycloid contained in the plane $\{x_3 = 0\}$, as we will explain next.

A *hypocycloid* of inner radius $r > 0$ and outer radius $R > r$ is the planar curve traced by a point on a circumference of radius r which is rolling along the interior of another circumference (which is fixed) of radius R. It can be parametrized by $\alpha(t) = (x(t), y(t))$, $t \in \mathbb{R}$, where

$$x(t) = -(R-r)\sin t + r\sin\left(\frac{R-r}{r}t\right), \quad y(t) = -(R-r)\cos t - r\cos\left(\frac{R-r}{r}t\right).$$

Using (24), we deduce that the image by X of the unit circle $\mathbb{S}^1 \subset \mathbb{C}$ has the following parametrization:

$$\theta \in [0, 2\pi) \mapsto X(e^{i\theta}) = \begin{pmatrix} -\frac{\sin(m\theta)}{m} + \frac{\sin((m+2)\theta)}{m+2} \\ -\frac{\cos(m\theta)}{m} - \frac{\cos(m+2)\theta}{m+2} \\ 0 \end{pmatrix}. \tag{25}$$

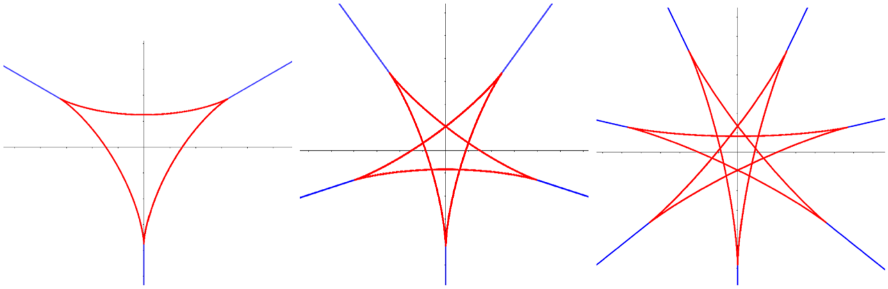

Figure 4. The intersection of H_m (with $m > 0$ even) with $\{x_3 = 0\}$ consists of a hypocycloid with $m+1$ cusps (in red) together with half-lines $\{tp \mid t \geq 1\}$ that start from each of these cusp points p. Left: $H_2 \cap \{x_3 = 0\}$, where the branch points have coordinates $(0, -\frac{3}{4}, 0), (-\frac{3\sqrt{3}}{8}, \frac{3}{8}, 0), (\frac{3\sqrt{3}}{8}, \frac{3}{8}, 0)$. Center: $H_4 \cap \{x_3 = 0\}$, Right: $H_6 \cap \{x_3 = 0\}$ (Color figure online)

From (25) we deduce that, up to the reparametrization $t = m\theta$, $X(\mathbb{S}^1)$ is the hypocycloid of inner radius $r = \frac{1}{m+2}$ and outer radius $R = \frac{2m+2}{m(m+2)}$, which has exactly $m+1$ cusps. These cusp points are the images by X of the $m+1$ branch points of H_m. In particular, H_m is the unique minimal surface obtained as solution of the Björling problem for the hypocycloid of $m+1$ cusps (this number of cusps is any odd positive integer, at least three), inner radius $r = \frac{1}{m+2}$ and outer radius $R = \frac{2m+2}{m(m+2)}$, when we take as normal vector field η (see Sect. 3 for the notation) the normal vector to the hypocycloid as a planar curve.

We depict this planar curve in the simplest cases $m = 2, 4, 6$ in Fig. 4 in red.

5.7. Revisiting the Case m Odd: H_m^* as a Solution of a Björling Problem for a Hypocycloid

Using the Weierstrass formula (1), it can be easily seen that the conjugate surface H_m^* of H_m with odd m can be parameterized in polar coordinates $z = re^{i\theta}$ by $X^*(re^{i\theta})$ given by the same formula as the right-hand-side of (24). $X^*(\mathbb{S}^1)$ parameterizes a hypocycloid γ_{2m+2} with inner radius $r = \frac{1}{m+2}$ and outer radius $R = \frac{2m+2}{m(m+2)}$. Since

$$\frac{R}{r} = \frac{2m+2}{m},$$

we deduce that γ_{2m+2} has $2m+2$ cusps.[2] Observe that $2m+2$ is a positive multiple of 4 because m is odd; and conversely, every positive multiple of 4 can be written as $2m+2$ for a unique $m \in \mathbb{N}$ odd. This tells us that for any $m \in \mathbb{N}$ odd, H_m^* is the unique solution to the Björling problem for the hypocycloid γ_{2m+2}, when we take as normal vector field η the normal vector to γ_{2m+2} as a planar curve.

Remark 8. 1. In the particular case of a hypocycloid of 4 cusps (called *astroid*), we recover the conjugate surface H_1^* of the classical Henneberg surface. This result was described by Odehnal [6], who also studied the Björling problem for an hypocycloid γ_3 of three cusps from the viewpoint of algebraic surfaces.

2. We have described the minimal surfaces obtained as the solution of a Björling problem over a hypocycloid if the number of its cusps is either any given odd number or a multiple of four. The case that remains is when the hypocycloid has $4k+2$ cusps, $k \in \mathbb{N}$. The corresponding solution to this Björling problem can be also explicitly described by the parametrization (24), now with a parameter $m \in \mathbb{Q}$. Namely, if we choose m to be of the form $m = \frac{1}{2k}$, $k \in \mathbb{N}$, inner radius $r = \frac{1}{m+2}$ and outer radius $R = \frac{2m+2}{m(m+2)}$, then
$$\frac{R}{r} = \frac{2m+2}{m} = 4k+2,$$
which ensures that the complete branched minimal surface $H_{\frac{1}{2k}} = X(\mathbb{C} \setminus \{0, \infty\})$ (here X is given by (24)) is symmetric by reflection in the (x_1, x_2)-plane), and $X(\mathbb{S}^1)$ is a hypocycloid with $4k+2$ cusps. $H_{\frac{1}{2k}}$ does not descend to a 1-sided quotient.

5.8. Isometries of H_m

As expected, the isometry group of H_m depends on whether m is even or odd.

Suppose firstly that <u>m is odd.</u> In this case, (23) gives:

(O1) The reflection of the z-plane about the imaginary axis, $re^{i\theta} \mapsto re^{i(\pi-\theta)}$, produces via X the reflectional symmetry about the (x_2, x_3)-plane in H_m.

(O2) The rotation $re^{i\theta} \mapsto re^{i(\theta+\pi+\frac{\pi}{m+1})}$ of angle $\pi + \frac{\pi}{m+1}$ about the origin in the z-plane, gives that H_m is symmetric under the rotation of angle $\frac{\pi}{m+1}$ about the x_3-axis composed by a reflection in the (x_1, x_2)-plane.

(O1), (O2) generate a subgroup of the extrinsic isometry group $\mathrm{Iso}(H_m)$ of H_m, isomorphic to the dihedral group D_{2m+2}.

[2] For a hypocycloid of inner radius $r > 0$ and outer radius $R > r$, the quotient R/r expresses the number of times that the inner circumference rolls along the outer circumference until it completes a loop. If R/r is a rational number and a/b is the irreducible fraction of R/r, then $b \cdot a/b = a$ counts the number of times that the inner circumference rolls until the point that generates the hypocycloid reaches its initial position. This number a coincides with the number of cusps.

Now assume that m is even. Using (24), we obtain:

(E1) The reflection $re^{i\theta} \mapsto re^{i(\pi-\theta)}$ of the z-plane about the imaginary axis produces via X the reflectional symmetry about the (x_2, x_3)-plane in H_m (this is a common feature of both the odd and even cases).

(E2) The rotation $re^{i\theta} \mapsto re^{i(\theta+\frac{2\pi}{m+1})}$ of angle $\frac{2\pi}{m+1}$ about the origin in the z-plane, gives that H_m is symmetric under the rotation of angle $\frac{2\pi}{m+1}$.

(E3) The antipodal map $re^{i\theta} \mapsto re^{i(\theta+\pi)}$ in the z-plane, produces a reflectional symmetry of H_m with respect to the (x_1, x_2)-plane.

(E1), (E2), (E3) generate a subgroup of $\mathrm{Iso}(H_m)$ isomorphic to the group $D_{m+1} \times \mathbb{Z}_2$.

Repeating the argument in the proof of Lemma 4, we now deduce the following.

Lemma 9. *Regardless of the parity of m, these are all the (intrinsic) isometries of H_m.*

6. Moduli Spaces of Examples with a Given Complexity

Our next goal is to analyze the structure of the family of solutions of the period problem with a given complexity in the sense of Definition 7. For $m = 1$, we will obtain uniqueness of the Henneberg surface H_1. This uniqueness is a special feature of the case $m = 1$, since continuous families of examples for complexities $m \geq 2$ can be produced.

We define the function $R\colon (0,\infty) \to (0,\infty)$, $R(r) = r - \frac{1}{r}$.

6.1. Solutions with Complexity $m = 1$

Since $m = 1$, solving the period problem (19) descending to the 1-sided quotient reduces to solving

$$\overline{cA_1} = -cA_3, \quad \mathrm{Im}(cA_2) = 0, \qquad -\frac{\overline{c}}{c} = \frac{a_1}{\overline{a_1}}\frac{a_2}{\overline{a_2}}. \tag{26}$$

Suppose that a list $(c, a_1, a_2) \in \mathbb{S}^1 \times (\mathbb{C}^*)^2$ is a solution of the 1-sided period problem, with associated branched minimal immersion X. Recall that $g(z) = z$ is its Gauss map. The list that gives rise to H_1 (Henneberg) is $(\pm 1, 1, i)$.

Remark 10. Since rotations of our surfaces are not allowed unless the rotation axis is vertical (see Remark 5) we can assume $a_1 \in \mathbb{R}^+$ from now on, although we cannot assume $a_1 = 1$.

Write a_1, a_2 in polar coordinates as $a_1 = r_1$, $a_2 = r_2 e^{i\theta_2}$, $r_1, r_2 > 0$, $\theta_2 \in [0, 2\pi)$. (18) can be written as

$$\begin{aligned} P(z) = {} & z^4 - \left[R(r_1) + R(r_2)e^{i\theta_2}\right] z^3 - \left[1 + e^{2i\theta_2} - R(r_1)R(r_2)e^{i\theta_2}\right] z^2 \\ & + \left[R(r_1)e^{2i\theta_2} + R(r_2)e^{i\theta_2}\right] z + e^{2i\theta_2}, \end{aligned}$$

hence

$$A_1 = R(r_1)e^{2i\theta_2} + R(r_2)e^{i\theta_2}, \tag{27}$$

$$A_2 = -\left[1 + e^{2i\theta_2} - R(r_1)R(r_2)e^{i\theta_2}\right], \tag{28}$$

$$A_3 = -\left[R(r_1) + R(r_2)e^{i\theta_2}\right]. \tag{29}$$

Writing $c = e^{i\beta}$, we have

$$\begin{aligned}
\overline{cA_1} + cA_3 &= R(r_1)\left[e^{-i(\beta+2\theta_2)} - e^{i\beta}\right] + R(r_2)\left[e^{-i(\beta+\theta_2)} - e^{i(\beta+\theta_2)}\right] \\
&= R(r_1)e^{-i\theta_2}\left[e^{-i(\beta+\theta_2)} - e^{i(\beta+\theta_2)}\right] - 2R(r_2)\sinh(i(\beta+\theta_2)) \\
&= -2e^{-i\theta_2}R(r_1)\sinh(i(\beta+\theta_2)) - 2iR(r_2)\sin(\beta+\theta_2) \\
&= -2i\left[R(r_1)e^{-i\theta_2} + R(r_2)\right]\sin(\beta+\theta_2), \qquad (30)\\
cA_2 &= -e^{i\beta}\left(1 + e^{2i\theta_2}\right) + R(r_1)R(r_2)e^{i(\beta+\theta_2)} \\
&= -e^{i(\beta+\theta_2)}\left(e^{-i\theta_2} + e^{i\theta_2}\right) + R(r_1)R(r_2)e^{i(\beta+\theta_2)} \\
&= -\left[2\cosh(i\theta_2) - R(r_1)R(r_2)\right]e^{i(\beta+\theta_2)} \\
&= -\left[2\cos\theta_2 - R(r_1)R(r_2)\right]e^{i(\beta+\theta_2)}. \qquad (31)
\end{aligned}$$

A list (c, a_1, a_2) solves the period problem if and only if the right-hand-side of (30) vanishes and the right-hand-side of (31) is real.

The third equation in (26) reduces to

$$e^{2i(\beta+\theta_2)} = -1. \tag{32}$$

Theorem 11. *The Henneberg surface H_1 is the only surface with $m = 1$ that solves the period problem and descends to a 1-sided quotient.*

Proof. By the above arguments, the right-hand-side of (30) vanishes, the right-hand-side of (31) is real and (32) holds.

(32) implies that $\sin(\beta + \theta_2) = \pm 1$. Since the right-hand-side of (30) vanishes, we have

$$R(r_1)e^{-i\theta_2} + R(r_2) = 0. \tag{33}$$

We have two possibilities:

- $r_1 = 1$. Thus (33) implies $r_2 = 1$. From, (32) we have $\beta + \theta_2 \equiv \pi/2 \mod \pi$ and from (31) we have $\cos\theta_2 = 0$, thus $\theta_2 = \pi/2$ or $\theta_2 = 3\pi/2$. This gives the lists $(1, 1, i)$, $(-1, 1, i)$, $(1, 1, -i)$ and $(-1, 1, -i)$. All of them give raise to the Henneberg surface.
- $r_1 \neq 1$. This implies $e^{-i\theta_2} = -\frac{R(r_2)}{R(r_1)}$, which is real. Hence $e^{-i\theta_2} = \pm 1$. As the function $r \mapsto R(r)$ is injective, this implies $r_1 = r_2$ and $\theta_2 = \pi$ or $r_2 = 1/r_1$ and $\theta_2 = 0$. Since the right-hand-side of (31) is real and (32) holds, $2\cos\theta_2 - R(r_1)R(r_2) = 0$. But in both cases $2\cos\theta_2 - R(r_1)R(r_2)$ does not vanish. Hence this possibility cannot occur.

□

6.2. Solutions with Complexity $m = 2$

Suppose that a list $(c = e^{i\beta}, a_1 = r_1, a_2 = r_2e^{i\theta_2}, a_3 = r_3e^{i\theta_3}) \in \mathbb{S}^1 \times \mathbb{R}^+ \times (\mathbb{C}^*)^2$ is a solution of the period problem with 1-sided quotient and associated branched minimal immersion X. The list that gives rise to H_2 is $(\pm i, 1, e^{i\pi/3}, e^{2i\pi/3})$.

Solving the period problem with 1-sided quotient is equivalent to solving

$$\overline{cA_2} = -cA_4, \quad \mathrm{Im}(cA_3) = 0, \quad -\frac{\overline{c}}{c} = \frac{a_2}{\overline{a_2}}\frac{a_3}{\overline{a_3}} \tag{34}$$

The third equation in (34) reduces to

$$e^{2i(\beta+\theta_2+\theta_3)} = -1. \tag{35}$$

(18) can be written as

$$P(z) = z^6 + A_5z^5 + A_4z^4 + A_3z^3 + A_2z^2 + A_1z + A_0,$$

where

$$\begin{aligned} A_2 &= e^{2i(\theta_2+\theta_3)} + e^{2i\theta_2} + e^{2i\theta_3} - R(r_1)R(r_2)e^{i(\theta_2+2\theta_3)} - R(r_1)R(r_3)e^{i(2\theta_2+\theta_3)} \\ &\quad -R(r_2)R(r_3)e^{i(\theta_2+\theta_3)}, \end{aligned} \tag{36}$$

$$\begin{aligned} A_3 &= 2\big[R(r_2)\cos\theta_3 + R(r_3)\cos\theta_2 + R(r_1)\cos(\theta_2-\theta_3) \\ &\quad -\frac{1}{2}R(r_1)R(r_2)R(r_3)\big]e^{i(\theta_2+\theta_3)}, \end{aligned} \tag{37}$$

$$\begin{aligned} A_4 &= -(1 + e^{2i\theta_2} + e^{2i\theta_3}) + R(r_1)R(r_2)e^{i\theta_2} \\ &\quad +R(r_1)R(r_3)e^{i\theta_3} + R(r_2)R(r_3)e^{i(\theta_2+\theta_3)}. \end{aligned} \tag{38}$$

Thus,

$$\overline{cA_2} + cA_4 = 2e^{-i[\beta+2(\theta_2+\theta_3)]}F, \tag{39}$$

$$cA_3 = \pm 2iG \tag{40}$$

where

$$F = e^{2i\theta_3} + \left[2\cos\theta_2 - R(r_1)R(r_2)\right]e^{i\theta_2} - R(r_3)\left[R(r_1) + R(r_2)e^{i\theta_2}\right]e^{i\theta_3}, \tag{41}$$

$$G = R(r_2)\cos\theta_3 + R(r_3)\cos\theta_2 + R(r_1)\cos(\theta_2-\theta_3) - \tfrac{1}{2}R(r_1)R(r_2)R(r_3). \tag{42}$$

Remark 12. (I) From (42) we deduce that G is real, hence the condition $\mathrm{Im}(cA_3) = 0$ only holds if and only if $G = 0$. We deduce that a list (c, a_1, a_2, a_3) solves the 1-sided period problem if and only if (35) holds and $F = G = 0$.

(II) The expression (41) is symmetric in $(r_2, \theta_2), (r_3, \theta_3)$. This can be deduced from the symmetry of A_2, A_4, or directly checked by using the equality

$$e^{2i\theta} = 2\cos\theta e^{i\theta} - 1, \qquad \theta \in \mathbb{R}, \tag{43}$$

which transforms (41) into

$$F = (1 + e^{2i\theta_2} + e^{2i\theta_3}) - R(r_1)\sum_{j=2}^{3} R(r_j)e^{i\theta_j} - R(r_2)R(r_3)e^{i(\theta_2+\theta_3)}. \quad (44)$$

Lemma 13. *If $F = 0$, then the coefficient of $R(r_1)$ in (44) is non-zero.*

Proof. Suppose $R(r_2)e^{i\theta_2}+R(r_3)e^{i\theta_3} = 0$. This leads to one of the following two possibilities: (a) $e^{i\theta_2} = e^{i\theta_3}$ and $R(r_2) = -R(r_3)$ or else (b) $e^{i\theta_2} = -e^{i\theta_3}$ and $R(r_2) = R(r_3)$. (a) implies $r_3 = 1/r_2$ and thus, (44) gives $F = 1+e^{2i\theta_2}(\frac{1}{r_2^2}+r_2^2)$. (b) implies $r_2 = r_3$ and (44) gives the same expression for F. In any case, we deduce from $F = 0$ that $e^{2i\theta_2}$ is real negative, hence $\frac{r_2^2}{r_2^4+1} = -e^{2i\theta_2} = 1$. This is impossible, since the function $x > 0 \mapsto \frac{x}{1+x^2}$ has a unique maximum at $x = 1$ with value $1/2$. □

The next result describes a one-parameter family of non-trivial examples of complexity $m = 2$ different from H_2.

Proposition 14. *Suppose that a list (c, a_1, a_2, a_3) solves the 1-sided period problem. Then:*

1. *If $r_1 = 1$, and at least one of r_2 or r_3 equals one, then $(c, a_1, a_2, a_3) = (\pm i, 1, e^{i\pi/3}, e^{2i\pi/3})$ and the example is H_2.*
2. *If $\theta_2 + \theta_3 = 0$ (mod π), then $r_2 = r_3$ or $r_2 = 1/r_3$ and (r_1, r_2) are given by the following functions of $\theta_2 \in (\frac{\pi}{4}, \frac{\pi}{3}] \cup [\frac{2\pi}{3}, \frac{3\pi}{4})$:*

$$R(r_1(\theta_2)) = \frac{1}{8\sqrt{2}}\frac{\sqrt{f(\theta_2) - 3}}{\cos\theta_2\cos(2\theta_2)}[f(\theta_2) + 3 + 4\cos(2\theta_2)], \quad (45)$$

$$R(r_2(\theta_2)) = -\frac{\sqrt{f(\theta_2) - 3}}{\sqrt{2}}, \quad (46)$$

or else (r_1, r_2) are given by the opposite expressions for both $R(r_1(\theta_2)), R(r_2(\theta_2))$, which exchange (r_1, r_2) by $(\frac{1}{r_1}, \frac{1}{r_2})$. Here, f is the function

$$f(\theta_2) = \sqrt{1 - 8\cos(2\theta_2) - 8\cos(4\theta_2)}. \quad (47)$$

Proof. If $r_1 = 1$, and at least one of r_2 or r_3 equals one, then (44) gives $1 + e^{2i\theta_2} + e^{2i\theta_3} = 0$ and (42) gives $R(r_2)\cos\theta_3 + R(r_3)\cos\theta_2 = 0$. Since at least one of r_2 or r_3 equals one, then at least one of R_2 or R_3 equals zero. In fact, both $R_2 = R_3 = 0$ (because otherwise we get $\cos\theta_2 = 0$ or $\cos\theta_3 = 0$, which prevents $1 + e^{2i\theta_2} + e^{2i\theta_3}$ from cancelling), and thus, $r_2 = r_3 = 1$. In this setting, $1 + e^{2i\theta_2} + e^{2i\theta_3} = 0$ leads to $(c, a_1, a_2, a_3) = (\pm i, 1, e^{i\pi/3}, e^{2i\pi/3})$, which proves item 1.

Now assume $\theta_2 + \theta_3 = 0$. Then (44),(42) give respectively

$$1 + 2\cos(2\theta_2) - R(r_2)R(r_3) = R(r_1)[R(r_2)e^{i\theta_2} + R(r_3)e^{-i\theta_2}], \quad (48)$$

$$(R(r_2) + R(r_3))\cos\theta_2 + R(r_1)\cos(2\theta_2) = \frac{1}{2}R(r_1)R(r_2)R(r_3). \quad (49)$$

Observe that $R(r_1)$ cannot vanish by Lemma 13 (another reason is that otherwise, (49) gives $\cos\theta_2 = 0$, and (48) gives $-1 - R(r_2)R(r_3) = 0$ which is absurd). From (48) we deduce that $R(r_2)e^{i\theta_2} + R(r_3)e^{-i\theta_2}$ is real. This implies that $[R(r_2) - R(r_3)]\sin\theta_2 = 0$. We claim that $\sin\theta_2 \neq 0$; otherwise $\theta_2 \equiv 0$ (mod π) and (48),(49) give the system

$$\begin{aligned} 3 - R(r_2)R(r_3) &= \pm R(r_1)[R(r_2) + R(r_3)], \\ R(r_1) \pm (R(r_2) + R(r_3)) &= \frac{1}{2}R(r_1)R(r_2)R(r_3), \end{aligned}$$

(with the same choice for signs), which can be easily seen not to have solutions.

Thus, $\sin\theta_2 \neq 0$ hence $R(r_2) = R(r_3)$ and $r_2 = r_3$. In this setting, (48),(49) reduce to

$$1 + 2\cos(2\theta_2) - R(r_2)^2 = 2R(r_1)R(r_2)\cos\theta_2, \tag{50}$$

$$2R(r_2)\cos\theta_2 + R(r_1)\cos(2\theta_2) = \frac{1}{2}R(r_1)R(r_2)^2. \tag{51}$$

If we assume $\theta_2 + \theta_3 = \pi$, then (44),(42) give respectively

$$1 + 2\cos(2\theta_2) + R(r_2)R(r_3) = R(r_1)[R(r_2)e^{i\theta_2} - R(r_3)e^{-i\theta_2}], \tag{52}$$

$$(-R(r_2) + R(r_3))\cos\theta_2 - R(r_1)\cos(2\theta_2) = \frac{1}{2}R(r_1)R(r_2)R(r_3). \tag{53}$$

Again, $R(r_1)$ can not vanish due to Lemma 13. From (52) we deduce that $R(r_2)e^{i\theta_2} - R(r_3)e^{-i\theta_2}$ is real. This implies that $[R(r_2) + R(r_3)]\sin\theta_2 = 0$. We claim that $\sin\theta_2 \neq 0$; otherwise $\theta_2 \equiv 0$ (mod π) and (52),(53) give the system

$$\begin{aligned} 3 + R(r_2)R(r_3) &= \pm R(r_1)[R(r_2) - R(r_3)], \\ -R(r_1) \pm (-R(r_2) + R(r_3)) &= \frac{1}{2}R(r_1)R(r_2)R(r_3), \end{aligned}$$

(with the same choice for signs), which again has no solutions. Thus, $\sin\theta_2 \neq 0$ hence $R(r_2) = -R(r_3)$ and $r_2 = 1/r_3$. In this setting, (48),(49) reduce again to (50) and (51).

The system (50),(51) has two equations and three unknowns r_1, r_2, θ_2. Next we describe its solutions. Consider the function f given by (47). Then,

$$f(\pi - \theta_2) = f(\theta_2), \text{ for each } \theta_2, \quad f(\theta_{2,0}) = 0 = f(\pi - \theta_{2,0}),$$

where $\theta_{2,0} = \frac{1}{2}\cot^{-1}\left(\frac{9}{\sqrt{32\sqrt{10}+95}}\right) \sim 0.499841$, and the domain of f is $[\theta_{2,0}, \pi - \theta_{2,0}] + \pi\mathbb{Z}$. The set $\{\theta_2 \in [\theta_{2,0}, \pi - \theta_{2,0}] \mid f(\theta_2) \geq 3\}$ equals $A := [\frac{\pi}{4}, \frac{\pi}{3}] \cup [\frac{2\pi}{3}, \frac{3\pi}{4}]$.

The unique solution (r_1, r_2) to the system (50),(51) as a function of θ_2 is given by (45), (46) and the opposite expressions for both $R(r_1(\theta_2)), R(r_2(\theta_2))$, which exchange (r_1, r_2) by $(\frac{1}{r_1}, \frac{1}{r_2})$. $\square$

6.2.1. The One-Parameter Family of Examples in Item 2 of Proposition 14. Observe that the map $\theta_2 \in (\frac{\pi}{4}, \frac{\pi}{3}] \mapsto \pi - \theta_2 \in [\frac{2\pi}{3}, \frac{3\pi}{4})$ is a diffeomorphism. Using the notation in item 2 of Proposition 14, for each $\theta_2 \in (\frac{\pi}{4}, \frac{\pi}{3}]$, we have

$$R(r_1(\pi - \theta_2)) = -R(r_1(\theta_2)), \qquad R(r_2(\pi - \theta_2))) = R(r_2(\theta_2)). \tag{54}$$

Each of these lists with $\theta_2 \in (\frac{\pi}{4}, \frac{\pi}{3}] \cup [\frac{2\pi}{3}, \frac{3\pi}{4})$ solves the 1-sided period problem, hence it defines a non-orientable, branched minimal surface $H(\theta_2)$. Furthermore, (54) implies that

$$r_1(\pi - \theta_2) = \frac{1}{r_1(\theta_2)}, \qquad r_2(\pi - \theta_2) = r_2(\theta_2). \tag{55}$$

We claim the surfaces $H(\theta_2)$ and $H(\pi - \theta_2)$ are congruent. To see this, note that the set of points $\{a_j, -1/\overline{a_j}\ \ j = 1, 2, 3\}$ that defines f through (16) and generates the surface $H(\theta_2)$, is:

$$\left\{ r_1, \frac{-1}{r_1}, r_2 e^{i\theta_2}, \frac{1}{r_2} e^{i(\pi+\theta_2)}, r_2 e^{-i\theta_2}, \frac{1}{r_2} e^{i(\pi-\theta_2)} \right\}. \tag{56}$$

The analogous set of points for the surface $H(\pi - \theta_2)$ is given through (55):

$$\left\{ \frac{1}{r_1}, -r_1, -r_2 e^{-i\theta_2}, \frac{1}{r_2} e^{-i\theta_2}, -r_2 e^{-i\theta_2}, \frac{1}{r_2} e^{i\theta_2} \right\},$$

which is up to sign the set described in (56). Therefore, the function f defined by equation (16) and the corresponding function $\widetilde{f}$ defined by the same formula for the surface $H(\pi - \theta_2)$ are related by $\widetilde{f}(-z) = -f(z)$, for each $z \in \mathbb{C}$. Using that $\omega = f\,dz$ and $\widetilde{\omega} = \widetilde{f}\,dz$ define, via the Weierstrass representation (1), related branched minimal immersions $X = (x_1, x_2, x_3)$ for $H(\theta_2)$ and $\widetilde{X} = (\widetilde{x}_1, \widetilde{x}_2, \widetilde{x}_3)$ for $H(\pi - \theta_2)$, we get that $H(\theta_2)$ and $H(\pi - \theta_2)$ are congruent.

In the sequel, we will reduce our study to the family $\{H(\theta_2) \mid \theta_2 \in (\frac{\pi}{4}, \frac{\pi}{3}]\}$. From (45), (46) we have

$$\lim_{\theta_2 \to \pi/3^-} R(r_1(\theta_2)) = \lim_{\theta_2 \to \pi/3^-} R(r_2(\theta_2)) = 0,$$

which implies that

$$\lim_{\theta_2 \to \pi/3^-} H(\theta_2) = H_2.$$

We next identify the limit (after rescaling) of the surfaces $H(\theta_2)$ as $\theta_2 \to \pi/4^+$. We first observe that

$$\lim_{\theta_2 \to \pi/4^+} R(r_1(\theta_2)) = -\infty, \qquad \lim_{\theta_2 \to \pi/4^+} R(r_2(\theta_2)) = 0. \tag{57}$$

This implies that the branch point $a_1 = a_1(\theta_2)$ is tending to zero, hence the limit of $H(\theta_2)$ when $\theta_2 \to \pi/4^+$ (if it exists) cannot be an example with complexity $m = 2$. Intuitively, it is clear than the complexity cannot increase when taking limits (even with different scales), hence by Theorem 11 it is natural to think that the limit of suitable re-scalings of $H(\theta_2)$ when $\theta_2 \to \pi/4^+$ be H_1. We next formalize this idea.

Another consequence of (57) is that the list $(c, a_1, a_2, a_3) = (i, r_1(\theta_2), r_2(\theta_2)e^{i\theta_2}, r_2(\theta_2)e^{-i\theta_2})$ converges as $\theta_2 \to \pi/4^+$ to $(c, a_1, a_2, a_3) = (i, 0, e^{i\pi/4}, e^{-i\pi/4})$. After applying to $H(\theta_2)$ a homothety of ratio $r_1(\theta_2) > 0$ (which shrinks to zero), the Weierstrass data of the shrunk surface $r_1(\theta_2)H(\theta_2)$ is $(g(z) = z,\ r_1(\theta_2)f(z))$, where $f(z)$ is given by (16). For $z \in \mathbb{C}\setminus\{0\}$ fixed,

$$
\begin{aligned}
&\lim_{\theta_2\to\pi/4^+} r_1(\theta_2)f(z) \overset{(16)}{=} \lim_{\theta_2\to\pi/4^+} r_1(\theta_2)\frac{i}{z^5}\prod_{j=1}^{3}(z-a_j)\left(z+\frac{1}{\overline{a_j}}\right)\\
&= \tfrac{i}{z^5}\left(z-e^{i\pi/4}\right)\left(z+e^{i\pi/4}\right)\left(z-e^{-i\pi/4}\right)\left(z+e^{-i\pi/4}\right)\lim_{\theta_2\to\pi/4^+}(z-r_1(\theta_2))\left(r_1(\theta_2)z+1\right)\\
&= \tfrac{i}{z^4}\left(z-e^{i\pi/4}\right)\left(z+e^{i\pi/4}\right)\left(z-e^{-i\pi/4}\right)\left(z+e^{-i\pi/4}\right) := \widehat{f}(z).
\end{aligned}
$$

Plugging the Weierstrass data $(g(z) = z\widehat{f}\,dz)$ into (1), we obtain a parametrization of the limit surface of $r_1(\theta_2)H(\theta_2)$ as $\theta_2 \to \pi/4^+$ in polar coordinates $z = re^{i\theta}$:

$$
\widehat{X}(re^{i\theta}) = \begin{pmatrix} \frac{-\sin\theta}{2}(r-\frac{1}{r}) + \frac{\sin(3\theta)}{6}(r^3-\frac{1}{r^3}) \\ -\frac{\cos\theta}{2}(r-\frac{1}{r}) - \frac{\cos(3\theta)}{6}(r^3-\frac{1}{r^3}) \\ -\cos\theta\sin\theta(r^2+\frac{1}{r^2}) \end{pmatrix}. \tag{58}
$$

We claim that this parametrization generates the Henneberg surface H_1. To see this, observe that if we first perform the change of variables $\theta = \widetilde{\theta} + \pi/4$ and then rotate the surface an angle of $-\frac{\pi}{4}$ around the x_3-axis, we get

$$
\begin{pmatrix} \cos\left(\frac{\pi}{4}\right) & \sin\left(\frac{\pi}{4}\right) & 0 \\ -\sin\left(\frac{\pi}{4}\right) & \cos\left(\frac{\pi}{4}\right) & 0 \\ 0 & 0 & 1 \end{pmatrix} \cdot \widehat{X}(re^{i(\widetilde{\theta}+\frac{\pi}{4})}) = -\begin{pmatrix} \frac{\cos\widetilde{\theta}}{2}(r-\frac{1}{r}) - \frac{\cos(3\widetilde{\theta})}{6}(r^3-\frac{1}{r^3}) \\ -\frac{\sin\widetilde{\theta}}{2}(r-\frac{1}{r}) - \frac{\sin(3\widetilde{\theta})}{6}(r^3-\frac{1}{r^3}) \\ \frac{\cos(2\widetilde{\theta})}{2}(r^2+\frac{1}{r^2}) \end{pmatrix},
$$

which is, up to a sign, the parametrization given in (6) for H_1 (see Fig. 5 for images of the surface $H(\theta_2)$ for three different values of $\theta_2 \in (\frac{\pi}{4}, \frac{\pi}{3}]$).

6.2.2. Around H_2 the Space of Examples with Complexity $m = 2$ is Two-Dimensional. Item 2 of Proposition 14 defines a non-compact family of non-orientable, branched minimal surfaces $\{H(\theta_2) \mid \theta_2 \in (\frac{\pi}{4}, \frac{\pi}{3}]\}$ inside the moduli space of examples with complexity $m = 2$. Apparently, the space of solutions for this complexity has real dimension 2 (the variables are $r_1, r_2, r_3, \theta_2, \theta_3$, $F = 0$ is a complex condition and $G = 0$ is a real condition). We can ensure this at least around H_2 via the implicit function theorem (this is consistent with item 2 of Proposition 14, since it imposes the extra condition $\theta_2 + \theta_3 = 0 \mod \pi$), as we will show next.

Consider the (smooth) period map given by

$$
\begin{aligned}
P: \quad (\mathbb{R}^+)^3 \times \mathbb{R}^2 &\longrightarrow \mathbb{R}^3 \equiv \mathbb{C} \times \mathbb{R} \\
((r_1, r_2), (r_3, \theta_2, \theta_3)) &\longmapsto (F(r_1, r_2, r_3, \theta_2, \theta_3), G(r_1, r_2, r_3, \theta_2, \theta_3)),
\end{aligned}
$$

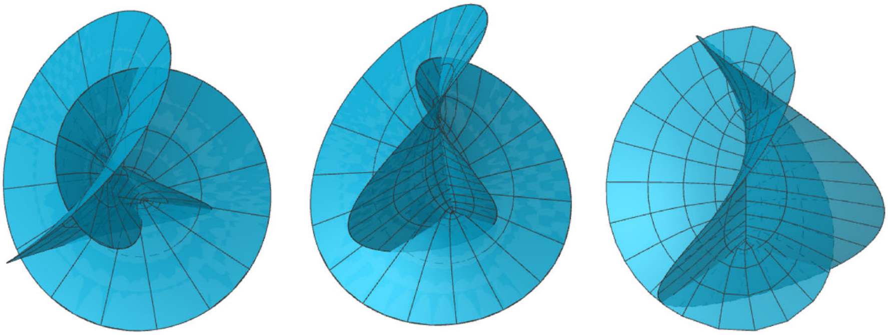

Figure 5. Surfaces generated by the previous lists $(c, a_1, a_2, a_3) = (i, r_1(\theta_2), r_2(\theta_2)e^{i\theta_2}, r_2(\theta_2)e^{-i\theta_2})$ with $\theta_2 = 1$ (left), $\theta_2 = 0.83$ (center), $\theta_2 = 0.7854$ (right). The limit of $r_1(\theta_2)H(\theta_2)$ as $\theta_2 \to \pi/4^+ \sim 0.785398$ is the Henneberg surface H_1

where F, G are given by (44), (42) respectively. Given $(r_1, r_2) \in (\mathbb{R}^+)^2$, let $P^{r_1,r_2} \colon \mathbb{R}^+ \times \mathbb{R}^2 \to \mathbb{R}^3$ be the restriction of P to $\{(r_1, r_2)\} \times \mathbb{R}^+ \times \mathbb{R}^2$. Then,

$$d(P^{r_1,r_2})_{(r_3,\theta_2,\theta_3)} \equiv \begin{pmatrix} \dfrac{\partial \mathrm{Re}(F)}{\partial r_3} & \dfrac{\partial \mathrm{Re}(F)}{\partial \theta_2} & \dfrac{\partial \mathrm{Re}(F)}{\partial \theta_3} \\ \dfrac{\partial \mathrm{Im}(F)}{\partial r_3} & \dfrac{\partial \mathrm{Im}(F)}{\partial \theta_2} & \dfrac{\partial \mathrm{Im}(F)}{\partial \theta_3} \\ \dfrac{\partial G}{\partial r_3} & \dfrac{\partial G}{\partial \theta_2} & \dfrac{\partial G}{\partial \theta_3} \end{pmatrix}. \tag{59}$$

Recall that the list associated to H_2 is $(r_1, r_2, r_3, \theta_2, \theta_3) = (1, 1, 1, \pi/3, 2\pi/3)$. Imposing this choice of parameters and computing the determinant of (59) we get

$$d(P^{1,1})_{(1,\pi/3,2\pi/3)} = 2\sqrt{3} \neq 0.$$

Thus, the implicit function theorem gives an open neighborhood $U \subset (\mathbb{R}^+)^2$ of $(r_1, r_2) = (1, 1)$, an open set $W \subset (\mathbb{R}^+)^3 \times \mathbb{R}^2$ with $(r_1, r_2, r_3, \theta_2, \theta_3) = (1, 1, 1, \pi/3, 2\pi/3) \in W$ and a smooth map $\varphi \colon U \to \mathbb{R}^3$ such that all the solutions $(r_1, r_2, r_3, \theta_2, \theta_3)$ around $(1, 1, 1, \pi/3, 2\pi/3)$ of the equation $P(r_1, r_2, r_3, \theta_2, \theta_3) = 0$ are of the form $(r_3, \theta_2, \theta_3) = \varphi(r_1, r_2)$. By Remark 12(I), the list

$$(c = e^{i\beta(r_1,r_2)}, r_1, r_2e^{i\theta_2}, r_3e^{i\theta_3})$$

with $\beta = \beta(r_1, r_2)$ given by (35) solves the 1-sided period problem and so, it defines a 1-sided branched minimal surface. This produces a 2-parameter deformation of the surface H_2 in the moduli space of examples with $m = 2$ around H_2, which in turn describes the whole moduli space around H_2.

Remark 15. A nice consequence of the classical Leibniz formula for the derivative of a product is a recursive law that gives the coefficients of the polynomial $P(z)$ defined by (18) in terms of the coefficients of the related polynomial for one complexity less. To obtain this recursive law, we first adapt the notation to the complexity:

$$P_{m+1}(z) := \prod_{j=1}^{m+1}(z - a_j)\left(z + \frac{1}{\overline{a_j}}\right) = \sum_{h=0}^{2m+2} A_{m+1,h} z^h. \tag{60}$$

(19) can now be written

$$\overline{cA_{m+1,m}} = -cA_{m+1,m+2}, \quad \mathrm{Im}(cA_{m+1,m+1}) = 0. \tag{61}$$

We want to find expressions for the above coefficients $A_{m+1,m}, A_{m+1,m+2}, A_{m+1,m+1}$, depending only on coefficients of the type $A_{m,h}$ (i.e., for one complexity less). Writing $a_j = r_j e^{i\theta_j}$ in polar coordinates, observe that

$$P_{m+1}(z) := P_m(z) Q_{m+1}(z), \quad \text{where } Q_{m+1}(z) = (z - r_{m+1}e^{i\theta_{m+1}})\left(z + \frac{e^{i\theta_{m+1}}}{r_{m+1}}\right).$$

Hence for $h \in \{m, m+1, m+2\}$,

$$A_{m+1,h} = \frac{1}{h!} P_{m+1}^{(h)}(0) = \frac{1}{h!}(P_m Q_{m+1})^{(h)}(0) = \frac{1}{h!}\sum_{k=0}^{h}\binom{h}{k} P_m^{(k)}(0) Q_{m+1}^{(h-k)}(0),$$

where in the last equality we have used Leibniz formula. Since Q_{m+1} is a polynomial of degree two, its derivatives of order three or more vanish. Hence we can reduce the last sum to terms where the index k satisfies $h - k \le 2$, i.e., $k \in \{h-2, h-1, h\}$ and thus,

$$\begin{aligned} A_{m+1,h} &= \frac{1}{h!}\Big[\tbinom{h}{h-2} P_m^{(h-2)}(0) Q''_{m+1}(0) + \tbinom{h}{h-1} P_m^{(h-1)}(0) Q'_{m+1}(0) + \tbinom{h}{h} P_m^{(h)}(0) Q_{m+1}(0)\Big] \\ &= \frac{1}{h!}\Big[\tfrac{h!}{(h-2)!2} P_m^{(h-2)}(0)\cdot 2 - h\, P_m^{(h-1)}(0) R(r_{m+1}) e^{i\theta_{m+1}} - P_m^{(h)}(0) e^{2i\theta_{m+1}}\Big] \\ &= \Big[\tfrac{1}{(h-2)!} P_m^{(h-2)}(0) - \tfrac{1}{(h-1)!} P_m^{(h-1)}(0) R(r_{m+1}) e^{i\theta_{m+1}} - \tfrac{1}{h!} P_m^{(h)}(0) e^{2i\theta_{m+1}}\Big] \\ &= A_{m,h-2} - A_{m,h-1} R(r_{m+1}) e^{i\theta_{m+1}} - A_{m,h} e^{2i\theta_{m+1}}, \end{aligned} \tag{62}$$

which is the desired recurrence law. (62) can be used to find solutions to (61) for complexity $m = 3$ besides the most symmetric example H_3, but the equations are complicated and we will not give them here.

Author contributions Both authors have contributed equally in the study.

Funding Funding for open access publishing: Universidad de Granada/CBUA This work is supported in part by the IMAG–Maria de Maeztu Grant CEX2020-001105-M/AEI/10.13039/501100011033, MICINN PID2020-117868GB-I00 and Junta de Andalucía P18-FR-4049 and A-FQM-139-UGR18.

Data availability Our manuscript has no associated data.

Declarations

Competing interests The authors have no relevant financial interests.

References

[1] do Carmo, M., Peng, C.K.: Stable complete minimal surfaces in $\mathbb{R}^3$ are planes. Bull. Am. Math. Soc. (N.S.) **1**, 903–906 (1979)

[2] Fischer-Colbrie, D., Schoen, R.: The structure of complete stable minimal surfaces in 3-manifolds of nonnegative scalar curvature. Commun. Pure Appl. Math. **33**, 199–211 (1980)

[3] Henneberg, L.: Über solche Minimalfläche, welche eine vorgeschriebene ebene Curve zur geodätischen Linie haben. Doctoral Dissertation, Eidgenössisches Polythechikum, Zurich (1875)

[4] Meeks III, W.H., Pérez, J.: Hierarchy structures in finite index CMC surfaces. Work in progress

[5] Micallef, M., White, B.: The structure of branch points in minimal surfaces and in pseudoholomorphic curves. Ann. Math. **141**(1), 35–85 (1995)

[6] Odehnal, B.: On algebraic minimal surfaces. KoG **20**, 61–78 (2016)

[7] Pogorelov, A.V.: On the stability of minimal surfaces. Sov. Math. Dokl. **24**, 274–276 (1981)

[8] Ros, A.: One-sided complete stable minimal surfaces. J. Differ. Geom. **74**, 69–92 (2006)

[9] Tysk, J.: Eigenvalue estimates with applications to minimal surfaces. Pac. J. Math. **128**, 361–366 (1987)

David Moya and Joaquín Pérez
Department of Geometry and Topology and Institute of Mathematics (IMAG)
University of Granada
Granada
Spain
e-mail: dmoya@ugr.es;
jperez@ugr.es

Received: July 5, 2022.
Accepted: December 23, 2022.